

III

Solar magnetism and large-scale flows

- Solar rotation from helioseismology
- The theory of differential rotation
- Evolution of large-scale and small-scale magnetic fields
- The solar dynamo
- Indicators of solar activity
- How typical is the Sun among solar type stars

The Sun's Internal Differential Rotation From Helioseismology

Philip R. Goode

Department of Physics
New Jersey Institute of Technology, Newark NJ, USA

Abstract: Well-confirmed helioseismic data from several groups using various observational techniques at different sites have allowed us to determine the differential rotation in the outer half of the Sun's interior. The resulting rotation law is simple – the surface differential rotation persists through much of the convection zone with a transition toward solid body rotation beneath. To date there is no appealing evidence for a rapidly rotating core. There is however, weak evidence for a solar cycle dependence of the Sun's internal rotation.

1. Introduction

Knowledge of the sun's internal rotation is a key to unlocking secrets of both solar evolution and the cause of surface activity. From helioseismology we have learned what we know about the Sun's internal rotation. Our seismic information comes from observations of intensity fluctuations in white light or Doppler shifts in a particular line. The oscillations discussed here are observed as the surface manifestation of trapped standing sound waves which sample the solar interior. Goldreich and Kumar (1989) have shown that these acoustic vibrations are apparently excited by turbulence in the outer most layers of the convection zone. The oscillations are global in nature and have a period of about five minutes. Global means that the lifetime of a mode is longer than the time it takes for the mode to circuit the part of the solar cavity it samples. Each normal mode samples its particular region of the interior and the seismology to be reviewed here is from oscillations which best sample between 0.5 and 0.9 R, where R is the solar radius. This choice is made because those data represent the only confirmed seismic data.

2. The nature of the oscillations

The solar oscillations are described by

$$\xi_{nlm}(r, \theta, \phi) = r \left[y(r), z(r) \frac{\partial}{\partial \theta}, z(r) \frac{1}{\sin \theta} \frac{\partial}{\partial \phi} \right] Y_l^m(\theta, \phi), \quad (1)$$

where the y_{nl} and z_{nl} are the radial and horizontal fluid displacement and ω is the angular frequency of the oscillation. The n, l and m quantum numbers are the radial order, angular degree and angular order respectively. The well-confirmed splitting data under consideration here are for l -values roughly between 10 and 100. In a high frequency asymptotic limit which is sufficiently valid in the five minute regime for us to gain insight to the oscillations, we can describe a unitless oscillation f by

$$f'' + f \left[\frac{\omega^2 r^2}{c^2} - l(l+1) + O\left(\left|\frac{d \ln \rho}{d \ln r}\right|^2, 1\right) \right] = 0, \quad (2)$$

where c is the local speed of sound. The inner turning point for the sound waves occurs when the first two terms in brackets are comparable. This means that the lower the degree of the oscillation the deeper it samples. On the other hand, near the surface where the speed of sound is low, the outer turning point is reached – for the intermediate l -values under consideration here – where the first term is comparable to the logarithmic derivative of the density. Thus the sampling depends on frequency rather than l . Since the five minute band is rather narrow, the oscillations sample the outer regions in the same way. This leads to the curious result that we know the rotation rate better at the base of the convection zone than near its top. If the Sun lacked perturbing forces like those due to rotation and magnetism then each (nl) -multiplet would be $(2l+1)$ -fold degenerate in m . The observers tell us that it is best to view the available data in (nl) -multiplets with a fine structure in m so that

$$\nu_{nlm} - \nu_{nlo} = L \sum_{i=1}^N a_{i,nl} P_i\left(\frac{m}{L}\right), \quad (3)$$

where P_i is a Legendre polynomial and $L = l$ or $\sqrt{l(l+1)}$ depending on the choice of the observer and $N = 5$ or 6 for now. The fact that equation (3) works implies that the perturbations manifest in the a -coefficients have the rotation axis as their axis of symmetry. If for instance, the Sun possessed an intense inclined magnetic field in its core, there would be difficulty in using equation (3) to describe the fine structure especially in multiplets which sample this region ($l < 5$). In detail, each multiplet would be characterized by at least $(2l+1)^2$ peaks per multiplet which is inconsistent with equation (3). The antisymmetric a -coefficients in equation (2) arise from the linear effect of rotation and the symmetric ones from shape distorting forces like the centrifugal force. The a_1 -, a_3 - and a_5 - terms are precisely correlated with a rotation law of the form

$$\Omega(r, \theta) = \Omega_0(r) + \Omega_1(r) \cos^2 \theta + \Omega_2(r) \cos^4 \theta, \tag{4}$$

where θ is the co-latitude. The inverse problem to determine $\Omega(r, \theta)$ follows from formally accounting for the effects of the Coriolis force and advection on the fine structure in the oscillation spectrum. In general, the three equations to determine $\Omega_0(r)$, $\Omega_1(r)$, and $\Omega_2(r)$ are coupled. However, the coupling is so weak that at the current level of accuracy in the five minute oscillation data the coupling can be safely ignored and

$$\frac{1}{2\pi} \int K_{nl}(r) \Omega_0(r) dr = a_{1,nl} + H_{03}(L) a_{3,nl} + H_{05}(L) a_{5,nl} \longrightarrow a_{1,nl} + a_{3,nl} + a_{5,nl} \tag{5}$$

$$\frac{1}{2\pi} \int K_{nl}(r) \Omega_1(r) dr = H_{13}(L) a_{3,nl} + H_{15}(L) a_{5,nl} \longrightarrow -5a_{3,nl} - 14a_{5,nl} \tag{6}$$

$$\frac{1}{2\pi} \int K_{nl}(r) \Omega_2(r) dr = H_{25}(L) a_{5,nl} \longrightarrow 21a_{5,nl} \tag{7}$$

where the $H(L)$ and angular integral coupling coefficients and the arrows indicate $L^2 \gg 1$. Examples of the $H(L)$ are given in Table 1. If $L^2 = l(l + 1)$ is chosen instead of $L = l$ then asymptotic limit is reached for lower l . The kernel, K_{nl} is

$$K_{nl}(r) = [y_{nl}^2(r) + l^2 z_{nl}^2(r) - 2y_{nl}(r)z_{nl}(r)] \rho r^4, \tag{8}$$

where ρ is the density.

Table 1. The $H(L)$ -coefficients

$L = l$					
l	$H_{25}(L)$	$H_{13}(L)$	$H_{15}(L)$	$H_{03}(L)$	$H_{05}(L)$
10	24.38	-5.46	-17.88	1.24	1.65
20	22.90	-5.24	-16.12	1.12	1.34
30	22.31	-5.16	-15.25	1.08	1.23
40	22.00	-5.12	-15.10	1.06	1.17
50	21.81	-5.10	-14.89	1.05	1.14
60	21.68	-5.08	-14.74	1.04	1.12
70	21.58	-5.07	-14.64	1.04	1.10
80	21.51	-5.06	-14.56	1.03	1.09
90	21.46	-5.05	-14.50	1.03	1.08
100	21.41	-5.05	-14.45	1.02	1.07
∞	21.00	-5.00	-14.00	1.00	1.00

$L = \sqrt{l(l + 1)}$					
l	$H_{25}(L)$	$H_{13}(L)$	$H_{15}(L)$	$H_{03}(L)$	$H_{05}(L)$
10	20.15	-4.97	-13.19	0.99	0.90
20	20.78	-4.99	-13.19	1.00	0.97
30	20.90	-5.00	-13.90	1.00	0.99
40	20.94	-5.00	-13.95	1.00	0.99

50	20.96	-5.00	-13.97	1.00	0.99
60	20.97	-5.00	-13.98	1.00	1.00
70	20.98	-5.00	-13.98	1.00	1.00
80	20.99	-5.00	-13.99	1.00	1.00
90	20.99	-5.00	-13.99	1.00	1.00
∞	21.00	-5.00	-14.00	1.00	1.00

3. The data

The resolved disk observational data have been used to determine the confirmed rotation laws. In these observations as many as 106 elements are used to detect oscillations. From these data splittings for l between 0 and 1000 can be determined in principle. The analysis proceeds by reducing the data into subspectra from which splittings can be identified. Even these projected spectra are quite complicated. Major complications arise from spatial and temporal sidebands which are a consequence of the fact that we observe only one side of the Sun and, to date, observe from a single site. To simplify the data reduction, many groups average their data over n . Libbrecht (1989) has shown that intrinsic linewidths of the peaks are sufficiently narrow that more accurate data will come from longer observing runs. Further, global networks like Global Oscillations Network Group (GONG) should provide data from multiple sites by the mid-1990s effectively eliminating the day-night temporal sidelobe problem. This network should yield data strings 10 time longer than the longest available now (~ 100 days). Nonetheless, there are several data sets currently available from which the internal rotation rate of the Sun has been determined. Some of the properties of these sets are given in Table 2. Each set provides data from somewhat different parts of the five minute spectrum – different in both l -range and frequency range. The data are from various observational groups using different instruments at several sites. Further, among

Table 2. The splitting data sets

	Epoch	Frequency Range(mHz)	Range in l	Averaged over n
Duvall <i>et al.</i> (1986)	1982.0	2.4 – 4.0	20–98	yes
Duvall and Harvey (1984)	1983.4	1.5 – 4.0	1–131	no
Tomczyk (1988)	1984.5	2.57–3.74	10–120	yes
Rhodes <i>et al.</i> (1987)	1984.6	2.2 – 3.6	3–89	yes
Brown and Morrow (1988)	1984.9	2.5 – 4.0	15–99	yes
Libbrecht (1989)	1986.5	1.5 – 4.0	10–60	no

the groups of observers, intensity and four different kinds of Doppler measurements were used as well as different reduction methods. Yet all the data are remarkably similar. The longest data string is that due to Libbrecht (1989). Further, this set is not averaged over n . As a result the most accurate inversions follow from these

data and extra attention is given to that set in this review. Splitting data results from that set are shown in Fig. 1.

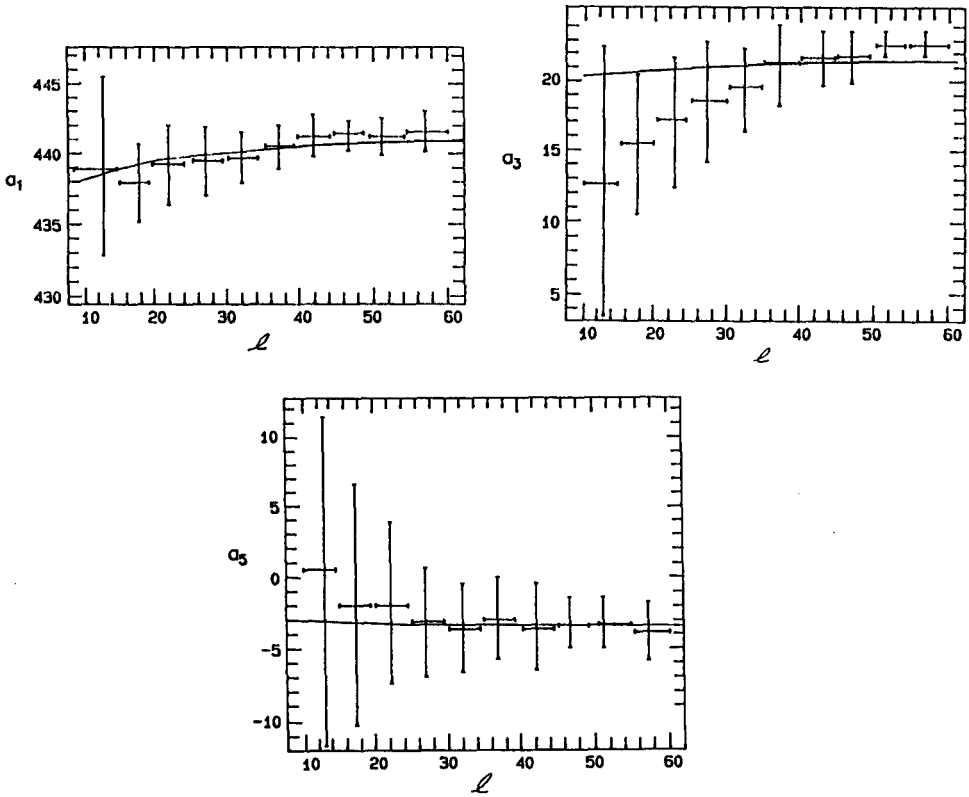


Fig. 1. Odd a -splitting coefficients (nHz) vs. l from Libbrecht's (1989) data. The solid line represents the determination of the coefficients from the mean rotation law of Eq. (9).

We have averaged the data over n and binned it in l for ease of viewing. We see that the a_1 are largely independent of l and have an average of about 440 nHz. The solid line through the a_1 data follows from assuming the mean rotation law from Libbrecht's (1989) data,

$$\Omega(r, \theta) = 460.2 \pm 0.2 - (58.3 \pm 1.3) \cos^2 \theta - (73.1 \pm 2.6) \cos^4 \theta. \quad (9)$$

This rotation law is quite close to that for the surface differential rotation. If we assumed rotation constant on cylinders instead, then the calculated a_1 varies between 420 and 430 nHz. The 420 nHz value applies for $l \sim 40$ where we know a_1 best. There the discrepancy is $\sim 10\sigma$. The a_3 coefficients average about 20 nHz. Their tendency to decrease with l results in rotation laws which show a decreased differential rotation with depth. The solid line is from a differential rotation which

does not decrease with depth. The a_5 -coefficient averages about -3 nHz and shows, perhaps, a trend for a_5 to increase toward zero with decreasing l . If we assume rotation constant on cylinders, the calculated a_3 and a_5 values would not be inconsistent with those from Eq. (9). From Fig. 1 it is clear that we know a_1 better than a_3 and a_3 better than a_5 . With this and Eqs. (5)–(7), we will know $\Omega_0(r)$ better than $\Omega_1(r)$ and $\Omega_1(r)$ better than $\Omega_2(r)$. Another way to understand why we know the rotation rate best in the Sun's equatorial plane is to recall that sectoral modes ($m = \pm l$) are the ones which are confined to that region of the solar interior. Thus, we could determine the equatorial rate by observing the spacing between $m = +l$ and $m = -l$ modes rather than the spacing between each of the $(2l + 1) - m$ peaks. The errors for each l would be reduced by a factor of $2l$ – the spacing between the two sectoral components.

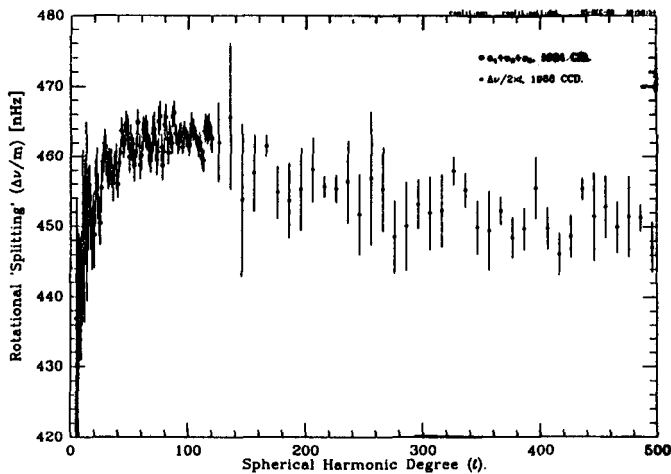


Fig. 2. $a_1 + a_3 + a_5$ (nHz) vs. l from the data of Rhodes *et al.* (1990b) for the $l=3$ –500 range.

The inner turning points for modes with $l = 10$ and 60 are about $0.3 R$ and $0.8 R$, respectively. Thus, it is clear that modes in the $l=10$ – 60 range clearly sample the region near the base of the convection zone. Considering the range of turning points, the asymptotic limits of Eqs. (5)–(7) and most importantly the data in Fig. 1, we anticipate the transition away from differential rotation with increasing depth. The detailed results are presented in the next section.

There are small differences between a_1 -, a_3 - and a_5 -coefficients from data set to data set. However the $a_1 + a_3 + a_5$ values are more robust from set to set suggesting that there is some residual correlation between the a -coefficients. This is also reflected in the fact that the first splitting data for the $l = 1$ –500 range are for $a_1 + a_3 + a_5$ only. These data are due to Rhodes *et al.* (1990b) and are those above $l=120$ are from 1988. The new high- l splitting data are consistent with but more accurate than the earlier sets due to Hill *et al.* (1988) and Deubner *et al.* (1979). The new high- l data are especially valuable in determining structure in

the rotation near the surface in the equatorial plane. The primary feature they reveal is a $\sim 5\%$ bump in Ω_0 centered at 0.93 R and having a width of about 0.1 R (Korzennik, 1990). However, this result must be regarded with caution because the bump in the splitting data centered near $l=80$ occurs where the sidelobes are very close to the "true" peaks.

For $l < 5$ whole disk observations should be useful. To date however, the limited results are contradictory. For instance, the reported rotational splitting for $l = 1$ by Jefferies *et al.* (1988) for the period of 1981–1984 is about 750 nHz implying a rapidly rotating core. On the other hand, Woodard (1984) reports an upper limit consistent with a core rotating more slowly than the surface in its equatorial region. Other results range between these two. Owing to this absence of consistency in the low- l splittings we do not use them in the calculation of the internal rotation.

Three groups have used whole disk observations to report the discovery of rotational splittings in gravity modes. Gravity modes are confined to the interior and such a discovery would enable a much more accurate seismology. Even though consistent splittings are reported by three groups indicating a rapidly rotating core, the groups also report significantly different identifications and frequencies for the g -modes. Until these discrepancies are cleared up, the identification of g -mode splittings should be regarded as unconfirmed. This situation is quite different than that for the acoustic modes for which the observers listed in Table 2 agree on the mode identifications and frequencies and their splittings. The SCLERA group reports rotational splittings which are about 3–4 times larger than any of the aforementioned splittings (Hill, 1984). This group observes fluctuations in the limb darkening function near the Sun's equator. The spectra are considerably more complicated than any of the spectra from aforementioned data.

We have well-confirmed rotational splitting data for acoustic modes in the five minute band for l -values in the 10–120 range. These facilitate the determination of the differential rotation between 0.4 R and 1.0 R.

4. The inversions

The typical approach to solving the inverse problem posed by equations (5)–(7) is a least squares one in which χ^2 per degree of freedom is minimized to determine the rotation rate. The problem here is that the data have a finite resolution width, and a gridding which is too fine will yield artificial short wavelength oscillations in the calculated rotation. The resolution width shown in Fig. 3 is for 0.7 R from Libbrecht's (1989) data using the Backus-Gilbert (1970) method. This least squares approach circumvents the problem of short wavelength oscillations but the cost is that the calculations require a large amount of time on a sizeable computer. The method employed here is regularization in which one minimizes α_s^2 , where

$$\alpha_s^2 = \chi_s^2 + \eta_s M_s P_s, \quad (10)$$

and where η_s is the regularization parameter and M_s is the number of (nl)-multiplets and

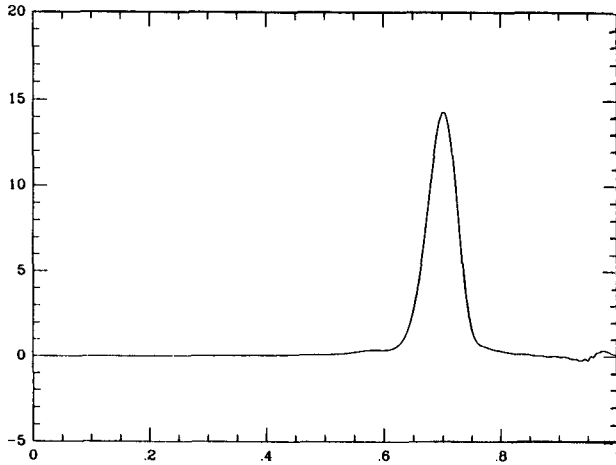


Fig. 3. Unitless Backus-Gilbert (1970) kernel for $0.70 R$ vs. fractional radius using the data of Libbrecht (1989).

$$P_s = \int \left| \frac{d\Omega_s}{dr} \right|^2 dr \tag{11}$$

and $s = 0, 1$ or 2 as in Eqs. (5)–(7). However, η_s is not a free parameter. The constraint invoked here reflects our *a priori* view that the rotation rate is a slowly varying function of radius. In the minimization of α_s^2 we vary η_s until χ_s^2 per degree of freedom is 1.

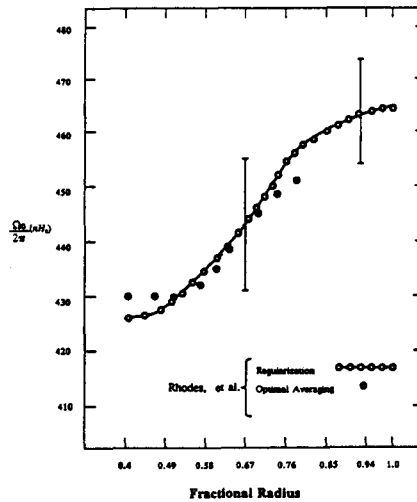


Fig. 4. $\frac{\Omega_s}{2\pi}$ vs. fractional radius from the data of Rhodes *et al.* (1987, 1990a).

Then the 1σ least square errors from the inversion are consistent with the 1σ errors in the data. In practice, the χ_s^2 -space is fairly flat and we further weaken η_s

until short wavelength oscillations almost begin to appear in the rotation. In Fig. 4, we see that $\Omega_0(r)$ calculated using the Backus-Gilbert (1970) approach compares favorably to that from regularization.

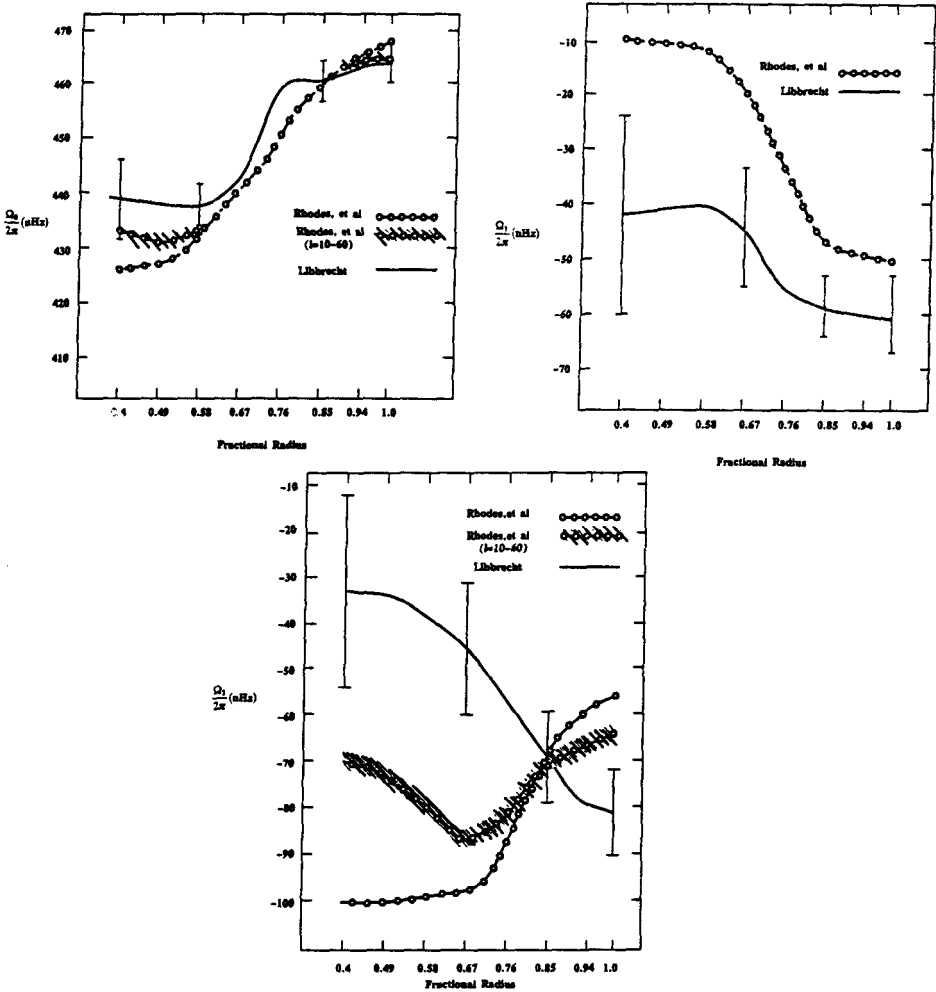


Fig. 5. $\frac{\Omega_0}{2\pi}$, $\frac{\Omega_1}{2\pi}$ and $\frac{\Omega_2}{2\pi}$ vs. fractional radius from Libbrecht's (1989) data. The errors from the Rhodes *et al.* (1987, 1990a) are about twice as large as those from Libbrecht's (1989) data. The shaded functions appear where the two rates from the Rhodes *et al.* (1987, 1990a) data differ.

In Fig. 5, we see the overall agreement for $\Omega_0(r)$, $\Omega_1(r)$, $\Omega_2(r)$ from Libbrecht's (1989) data and those from Rhodes *et al.* (1987, 1990a) data for $l=3-89$ and its $l=10-60$ subset. The error bars on the full Rhodes *et al.* (1987, 1990a) data set are about twice those from Libbrecht's reflecting the fact that Rhodes *et al.* averaged over n and their observation run has fewer days in it. The $\Omega_0(r)$ functions tend to be flat through the convection zone with a sharp gradient below. It seems

though that the sharpness of the gradient depends on which data are excluded. Near the surface, as mentioned earlier, the Rhodes *et al.* (1990b) data yielded a bump in $\Omega_0(r)$ near 0.93R. However that rate is fairly flat throughout the rest of the convection zone showing a decreasing rate going inwards like that in Fig. 5 from the data of Libbrecht. The decrease beneath the bump starts near the base of the convection zone. The low- l data are not so secure so it is not clear whether or not $\Omega_0(r)$ continues to decline beneath 0.6 R. For $\Omega_1(r)$ both sets show a strong tendency away from differential rotation beneath the convection zone. For $\Omega_2(r)$ the results are consistent at the 1σ level in the least square error bars, while showing opposite trends. The function $\Omega_2(r)$ is not yet well determined.

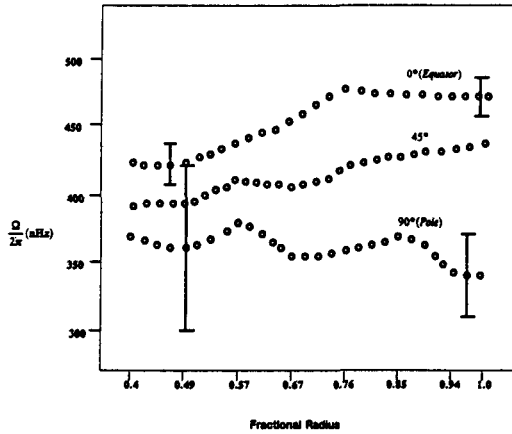


Fig. 6. $\frac{d\Omega}{dt}$ at three latitudes vs. fractional radius from the data of Tomczyk (1988).

Nonetheless, the net tendency away from the surface like differential rotation is clear and is arbitrarily illustrated with the $l=10-120$ splitting data of Tomczyk (1988). Regularization oversmooths the rotation rate and so the gradients in $\Omega_0(r)$ and $\Omega_1(r)$ could be even sharper than they appear in Fig. 4. Fig. 7 shows the results from Libbrecht's (1989) data of allowing a discontinuity at 0.73 R, near the base of the convection zone. The striking result is surface-like differential rotation throughout the convection zone with an abrupt transition to solid body rotation beneath at a rate close to mid-latitude surface rate. Moving the arbitrary discontinuity either closer to or further from the surface results in a reduction in magnitude of the jump. In fact, the jump essentially vanishes if the arbitrary discontinuity is moved by 0.1R in either direction. Of course Fig. 7 is only a curiosity because of the limited resolving power of the data as illustrated in Fig. 2. Owing to the resolving power we do not pay a high price for the oversmoothing of regularization. To further illustrate the accuracy to which we know the rotation we try a second constraint

$$P_s = \int \left| \frac{d^2 \Omega_s}{dr^2} \right|^2 dr \tag{12}$$

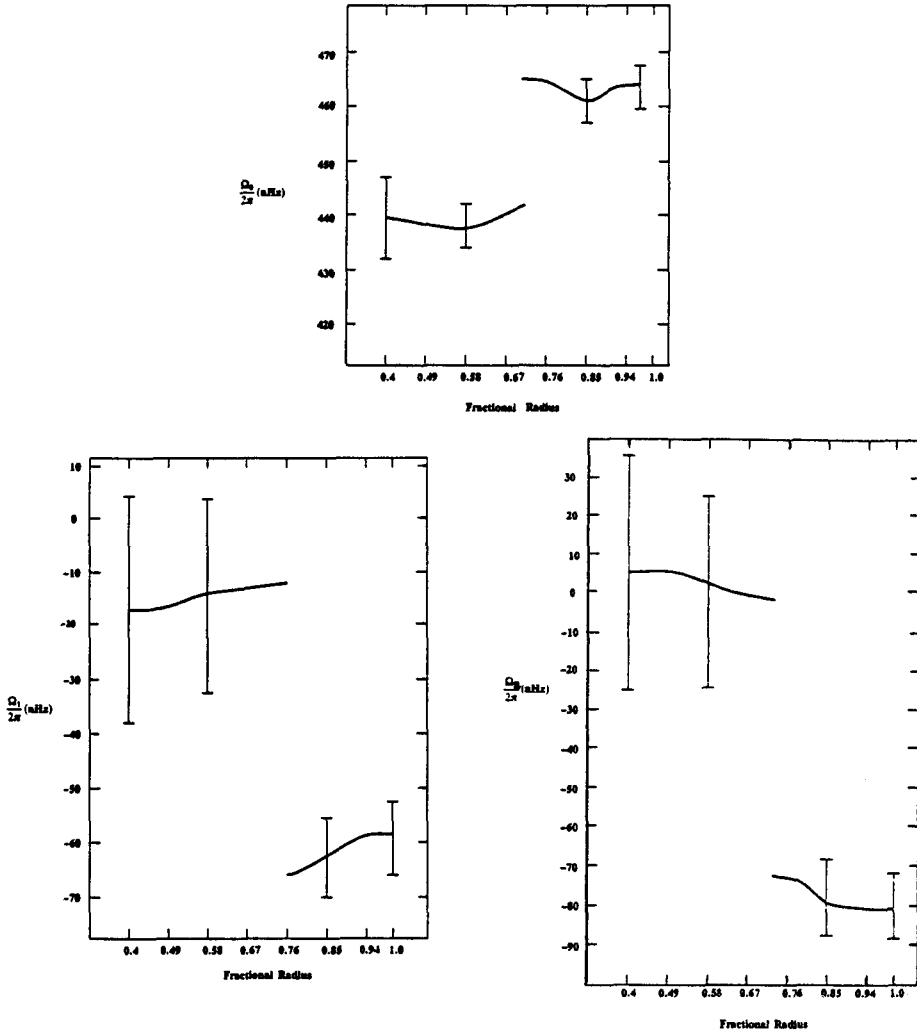


Fig. 7. $\frac{\Omega_0}{2\pi}$, $\frac{\Omega_1}{2\pi}$ and $\frac{\Omega_2}{2\pi}$ vs. fractional radius from Libbrecht's (1989) data allowing a discontinuity at 0.73 R.

In Fig. 8, the results of this constraint are compared to that of equation (11) for the data of Libbrecht. For $\Omega_0(r)$, the results are the same except that, not surprisingly, the gradient in Ω_0 is larger near the base of the convection zone. For the two $\Omega_1(r)$ results the trends are the same but the role of the constraint is larger here. The $\Omega_2(r)$ functions are controlled by the constraints. The first determination of the Sun's internal rotation was made by Duvall *et al.* (1984). That inversion for the rotation near the equatorial plane is largely consistent with the $\Omega_0(r)$ values here. However, the results also suggested the hint of a rapidly rotating core. That hint is probably an artifact of the previously discussed short wavelength oscillations in rotation resulting from too fine a grid in $\Omega_0(r)$. In Fig. 9, regularized inversions

are compared with η_0 for Figures 4–7 to that from a much smaller η_0 with a step size of $0.05 R$. The latter solution roughly shows the form given by Duvall *et al.* (1984) including the dip near $0.3R$ and the rapidly rotating core. As η_0 is increased from the too small value to a reasonable one, first the oscillations near the center disappear then those near the surface disappear.

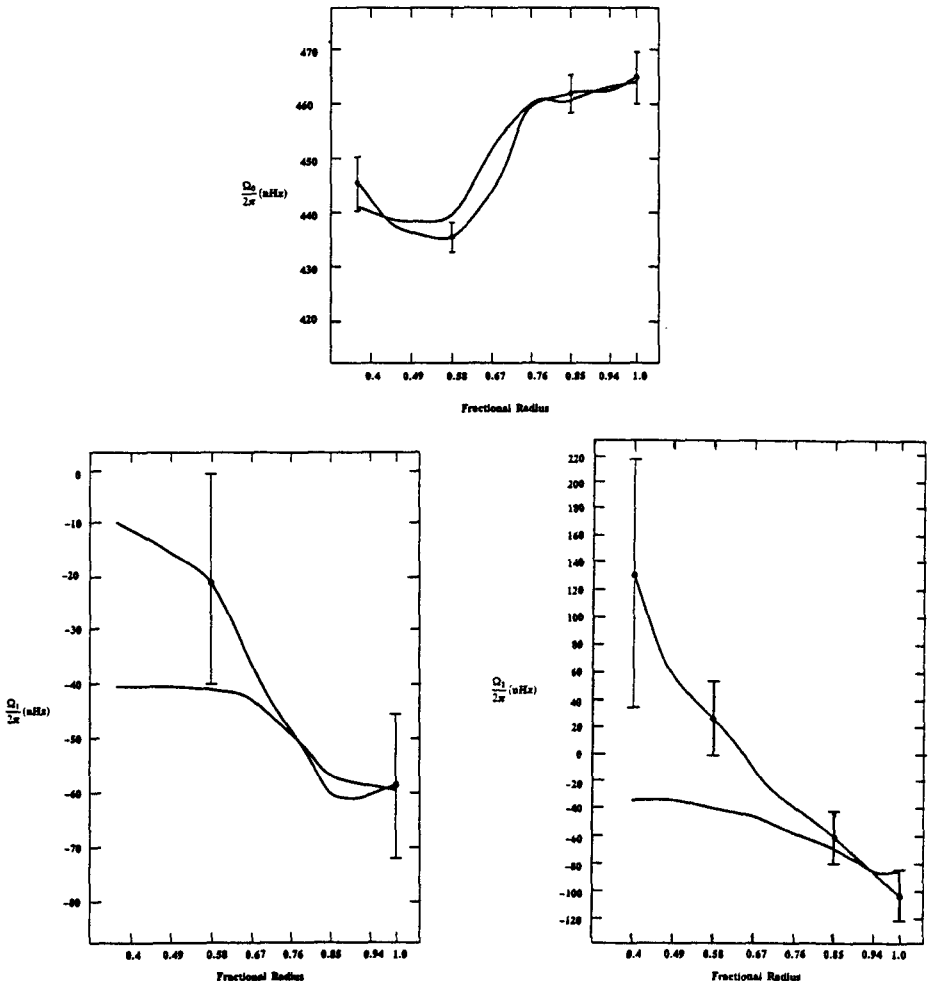


Fig. 8. $\frac{\Omega_0}{2\pi}$, $\frac{\Omega_1}{2\pi}$ and $\frac{\Omega_2}{2\pi}$ vs. fractional radius from the data of Libbrecht (1989). The error bars are on the inversion using the constraint of Eqs. (12).

5. Is the internal rotation time dependent?

We have rotation splitting data from the last solar maximum until now. The only change in rotation that appears to be marginally significant is in Ω_0 in the radiative interior (Goode *et al.*, 1991; Goode and Dziembowski, 1991) near 0.4 R. The rate at that location appears to be anticorrelated with surface activity as shown in Fig. 10. In detail, that rate was maximal at solar minimum.

Further, Ω_0 near the base of the convection zone does not appear to change at all over the cycle. Dziembowski and Goode (1991) inverted the symmetric part of preliminary oscillation data of Libbrecht and Woodard (1990) from the summer of 1986 and 1988 to determine that there appears to be a persistent megagauss quadrupole toroidal field near the base of the convection zone. Such a field is too intense to vary over the activity cycle. In an effort to rationalize these apparently disparate and marginally significant effects of rotation and magnetism, Goode and Dziembowski (1991) suggested the possibility of a torsional oscillation vaguely like that suggested years ago by Walen (1947).

The rationalization is a picture in which the megagauss field is maintained by a dynamo action on an "invisible" constant kilogauss poloidal field near the base of the convection zone. The equation of motion for the torsional oscillation is

$$\rho r^2 \sin^2 \theta \frac{\partial^2 \Omega}{\partial t^2} = \frac{1}{4\pi} (\mathbf{B}_p \cdot \nabla) [r^2 \sin^2 \theta (\mathbf{B}_p \cdot \nabla) \Omega] \quad (13)$$

where \mathbf{B}_p is the poloidal field and its kilogauss magnitude is chosen so that the torsional oscillation has a period comparable to that of the activity cycle. The dynamo action generating the toroidal field, \mathbf{B}_ϕ , is described by

$$\frac{\partial \mathbf{B}_\phi}{\partial t} = r \sin \theta (\mathbf{B}_p \cdot \nabla) \Omega. \quad (14)$$

Since we expect the time dependent dynamo to be amplitude limited, the larger B_p is the smaller amplitude variation in Ω over time. Thus, we would expect that the rotation rate near the base of the convection zone would change much less than the rate deep down where B_p would be considerably smaller. Of course there are problems with this picture, like how would the rotational energy stored deep down, even after conversion to magnetic energy, be transferred to the surface over 11 years.

6. Conclusions

Various groups of observers have collected several sets of consistent splitting data spanning overlapping regions of the five minute period acoustic band. These data have been used to infer that the surface rate at any point persists through the convection zone going inward along the radius from the chosen point. Near the base of the convection zone there is a fairly abrupt transition towards solid body

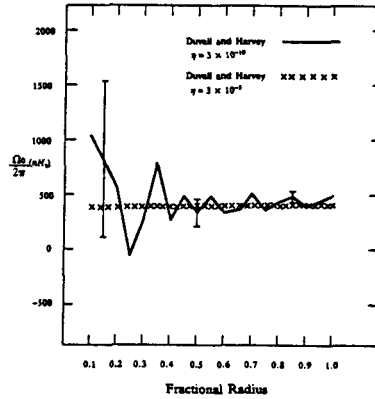


Fig. 9. $\frac{\Omega_0}{2\pi}$ vs. fractional radius from the data of Duvall and Harvey (1984) mimicking the calculation of Duvall *et al.* (1984). For the smooth function the error bars are comparable to the width of the x's.

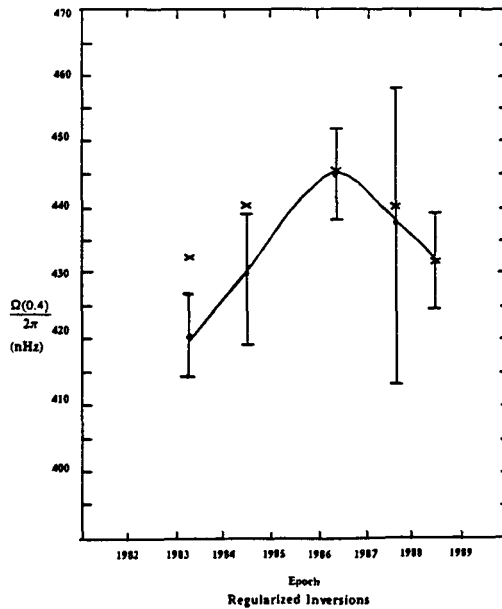


Fig. 10. $\frac{\Omega_0(r=0.4R)}{2\pi}$ vs. epoch. The x's represent the inverse sunspot number calibrated between 1986.5 and 1988.5.

rotation beneath. The solid body rate is close to that of an intermediate surface latitude. Brown *et al.* (1989) and Dziembowski *et al.* (1989) used the confluence of the radial and latitudinal gradients to suggest that the dynamo driving solar activity is seated near the base of the convection zone. The rotation law in the convection zone is not consistent with rotation on cylinders as suggested by detailed treatments of the consequences of turbulent convection on solar activity. Nonetheless, we should be encouraged because the rotation law is simple. We need

to search for the dynamical origin of this simple law. In the near future we expect to know the Sun's internal differential rotation about ten times more accurately than we know it now because of projects like GONG as well as observations from space.

P.R.G is partly supported by AFOSR 89-0048.

References

- Backus, G., Gilbert, F.: 1970, *Phil. Trans. Roy. Soc. London, A* **266**, 123
- Brown, T.M., Christensen-Dalsgaard, J., Dziembowski, W.A., Goode, P.R., Gough, D.O., Morrow, C.A.: 1989, *Astrophys. J.* **343**, 526
- Brown, T.M., Morrow, C.A.: 1987, *Astrophys. J. Letters* **314**, 121
- Deubner, F.L., Ulrich, R.K., Rhodes, E.J.: 1979, *Astron. Astrophys.* **72**, 177
- Duvall, T.L., Dziembowski, W.A., Goode, P.R., Gough, D.O., Harvey, J.W., Leibacher, J.W.: 1984, *Nature* **310**, 22
- Duvall, T.L., Harvey, J.W.: 1984, *Nature* **310**, 19
- Duvall, T.L., Harvey, J.L., Pomerantz, M.A.: 1986, *Nature* **321**, 500
- Dziembowski, W.A., Goode, P.R.: 1991, *Astrophys. J.*, in press.
- Dziembowski, W.A., Goode, P.R. and Libbrecht, K.G.: 1989, *Astrophys. J. Letters* **337**, L53
- Goldreich, P., Kumar, P.: 1988, *Astrophys. J.* **326**, 462
- Goode, P.R., Dziembowski, W.A.: 1991, *Nature*, in press.
- Goode, P.R., Dziembowski, W.A., Korzennik, S.G., Rhodes, E.J.: 1991, *Astrophys. J.*, in press.
- Hill, F., Gough, D.O., Toomre, J. and Haber, D.A.: 1988, in *Advances in Helio- and Asteroseismology*, IAU Symposium No. 123, ed. J. Christensen Dalsgaard and S. Frandsen, Dordrecht, Reidel, p. 45
- Hill, H.A.: 1984, SCLERA Monograph Series, No. 1.
- Jefferies, S.M., McLeod, C.P., Van der Raay, H.B., Palle, P.L., Roca Cortes, T.: 1988, in *Advances in Helio- and Asteroseismology*, IAU Colloquium 123, ed. J. Christensen Dalsgaard and S. Frandsen, Dordrecht, Reidel, p. 25
- Korzennik, S.G.: 1990, Ph.D. dissertation, University of California at Los Angeles, in preparation.
- Libbrecht, K.G.: 1989, *Astrophys. J.* **336**, 1092
- Libbrecht, K.G., Woodard, M.: 1990, *Nature* **345**, 779 and private communication
- Rhodes, E.J., Cacciani, A., Korzennik, S., Tomczyk, S., Ulrich, R.K., Woodard, M.F.: 1990a, *Astrophys. J.*, in press.
- Rhodes, E.J., Cacciani, A., Woodard, M.F., Tomczyk, S., Korzennik, S., Ulrich, R.K. 1987, in *The Internal Solar Angular Velocity*, eds. B.R. Durney and S. Sofia, Dordrecht, Reidel, p. 75
- Rhodes, E.J., Korzennik, S., Ulrich, R.K.: 1990b, in preparation.
- Tomczyk, S.: 1988, Ph.D. dissertation, University of California at Los Angeles.
- Walen, C.: 1947, *Ark. Mat. astr. Fys.* **33a**, 1
- Woodard, M.F.: 1984, *Nature* **309**, 530